

Can Oceanic Freshwater Flux Amplify Global Warming?

LIPING ZHANG AND LIXIN WU

Physical Oceanography Laboratory, Ocean University of China, Qingdao, China

(Manuscript received 28 March 2011, in final form 21 November 2011)

ABSTRACT

The roles of freshwater flux (defined as evaporation minus precipitation) changes in global warming are studied using simulations of a climate model in which the freshwater flux changes are suppressed in the presence of a doubling of CO₂ concentration. The model simulations demonstrate that the warm climate leads to an acceleration of the global water cycle, which causes freshening in the high latitudes and salinification in the subtropics and midlatitudes. It is found that the freshwater flux changes tend to amplify rather than suppress global warming. Over the global scale, this amplification is largely associated with high-latitude freshening in a warm climate, which leads to a shoaling of the mixed layer depth, a weakening of the vertical mixing, and thus a trapping of CO₂-induced warming in the surface ocean. The latitudinal distribution of SST changes due to the effects of freshwater flux changes in a warm climate is complicated, involving anomalous advection induced by both salinity and wind stress changes. In addition, atmospheric feedbacks associated with global warming also amplify the SST warming.

1. Introduction

Both observations and climate models indicate that the freshwater flux [defined as evaporation minus precipitation (EmP)] exhibits substantial changes as a consequence of global warming (e.g., Curry et al. 2003). Dai et al. (1997) demonstrated an increasing trend in the global mean precipitation over the land between 1900 and 1988. Wong et al. (1999) pointed out that the precipitation over the high-latitude oceans increases notably between 1930 and 1980 and 1985 and 1994 based on the salinity measurements of the intermediate waters. Furthermore, all climate models predict an intensification of the ocean water cycle in response to increased greenhouse gases (Cubasch et al. 2001; Williams et al. 2007; Seager and Naik 2010).

The changes of the ocean water cycle directly lead to changes in water vapor, which acts as a dominant greenhouse gas and provides the largest known feedback to amplify global warming. Both observational and modeling studies so far have focused on changes of water vapor concentration and feedback to climate (e.g., Hall and Manabe 1999; Soden 2000; Soden et al. 2002,

2005). In addition to the water vapor feedback, salinity anomalies induced by changes in the ocean water cycle may also modulate large-scale ocean circulation and climatic responses to global warming. The changes in salinity can lead to density and stratification changes in the upper ocean, which can affect both wind-driven and thermohaline circulations, and thus oceanic heat sequestration and transport (e.g., Fedorov et al. 2007). However, the processes and mechanisms have not been well understood.

Salinity can be an important gauge of the global water cycle. Lukas and Santiago-Mandujano (2008) use the long-time series station offshore Hawaii to examine the relationship between salinity changes and variations in surface freshwater fluxes in the North Pacific, and found that deep salinity layers can record the surface freshwater extent as they are subducted into the thermocline. In addition, salinity anomalies are long-lived active tracers, which can be transported from region to region, and thus may play a more important role in long-term climate variability (Zhong and Liu 2009).

Recent modeling studies advance our understanding of the role of salinity in large-scale ocean circulation and climate changes. Ocean general circulation models forced with idealized freshwater flux anomalies in low latitudes reveal basin-scale changes in temperature, salinity, and circulation (Huang and Mehta 2005; Huang et al. 2005). Fedorov et al. (2004) suggested that freshening

Corresponding author address: Dr. Lixin Wu, Physical Oceanography Laboratory, Ocean University of China, 5 Yushan Road, Qingdao 266003, China.
E-mail: lxwu@ouc.edu.cn

in the northern extratropics can deepen the equatorial thermocline due to a reduction of the subtropical–tropical cell. Our coupled model studies further demonstrate that recent freshwater flux loss over the Kuroshio–Oyashio Extension and the Gulf Stream extension can not only induce basin-scale changes in SST and circulations but also trigger interbasin interactions by atmospheric teleconnection and oceanic bridge (Zhang et al. 2011a,b). These modeling studies basically focus on the impacts of regional freshwater flux and salinity changes. Using a fully coupled GCM by artificially changing the freshwater flux, Williams et al. (2006, 2007) suggested that an amplified global water cycle may lead to cooling over the global ocean due to an increased vertical component of the isopycnal diffusive heat flux. This potentially points to a negative feedback of freshwater flux in global warming, which may partly offset the positive feedback of water vapor due to the amplification of the water cycle in global warming.

While the idealized modeling result of Williams et al. (2006, 2007) is intriguing, its relevance to global warming needs to be further assessed because in their modeling studies, the CO_2 concentration remains the same in both the control run (CTRL) and the sensitivity experiment. A different CO_2 concentration may lead to different sensitivity of large-scale ocean circulation and climate to salinity changes. In this paper, we extend the modeling study of Williams et al. (2006, 2007) by fixing the freshwater flux to the model climatology in a fully coupled ocean–atmosphere model with a doubling of CO_2 concentration. We find that salinity changes induced by freshwater flux changes tend to enhance rather than reduce the amplitude of global warming.

The paper is arranged as follows. Section 2 briefly describes the coupled model and experimental setup. Section 3 studies the responses and mechanisms of both global and regional SST to salinity changes in global warming. A summary and some further discussions are given in section 4.

2. Model and experimental design

We use the Fast Ocean Atmosphere Model (FOAM) version 1.5, a fully coupled model developed at the University of Wisconsin. This is an improved version of the original FOAM (version 1.0), which was described in detail in Jacob (1997). The atmospheric model is a parallel version of the National Center for Atmospheric Research (NCAR) Community Climate Model version 2 (CCM2) but with the atmospheric physics replaced with those of CCM3. The ocean model was developed following the Geophysical Fluid Dynamics Laboratory (GFDL) Modular Ocean Model (MOM). The FOAM

version used here has an atmospheric resolution of R15 but with 18 vertical levels and an oceanic resolution of $1.4^\circ \times 2.8^\circ$ with 32 vertical levels. Without flux adjustment, the fully coupled model has been integrated for over 2000 yr without an apparent climate shift. FOAM reasonably captures features of the observed climatology (Jacob 1997; Zhang et al. 2011a), as well as some climate variability modes, including ENSO (Liu et al. 2000) and Pacific decadal climate variability (Wu et al. 2003).

The responses of freshwater water flux and salinity to a doubling of CO_2 simulated by FOAM are similar to most of the climate models used for the Intergovernmental Panel on Climate Change (IPCC) Fourth Assessment Report (AR4). Both EmP and the salinity anomaly patterns of the ensemble mean of the IPCC AR4 models and FOAM are broadly similar to the climatological patterns: positive (salinification) in the subtropical and negative (freshening) in the high-latitude oceans, implying an amplification of the water cycle in global warming (Fig. 1). In the tropical Pacific, the FOAM-simulated EmP anomalies have a broader scale and weaker amplitude than the ensemble mean of the IPCC AR4 models. Despite these differences in the tropics, the responses induced by freshwater flux changes are found most significantly in the high-latitude oceans, where FOAM and the IPCC AR4 models display consistent EmP changes in both magnitude and pattern.

To assess the effects of oceanic freshwater flux changes in global warming, we conduct two groups of global warming experiments, with each group consisting of two parallel runs. The first group includes a CTRL with a normal CO_2 concentration (385 ppm) and a run with a doubled- CO_2 concentration (2CO_2). The second group is configured the same as for the first group but with the EmP flux fixed to the mean seasonal cycle of the CTRL in both the normal and the doubled- CO_2 runs (2CO_2 _FixEmP). In principle, it is not necessary to run a fixed EmP experiment with the normal CO_2 concentration in the second group. Here, this run serves as a control run for the 2CO_2 _FixEmP experiment to minimize the errors potentially caused by model climate drift due to a fixed EmP flux in the coupled run. Note that the fixed EmP flux is only applied to the ocean salinity equation in the form of virtual salinity flux. This type of experimental setup deliberately leaves the latent heat flux and associated water vapor unconstrained to preserve the global surface heat and moisture balance, and thus allows us to focus solely on the salinity impacts. Each experiment is integrated for 300 yr and the last 100 yr are averaged for analysis. The responses are taken as the differences between the global warming run and its corresponding control run.

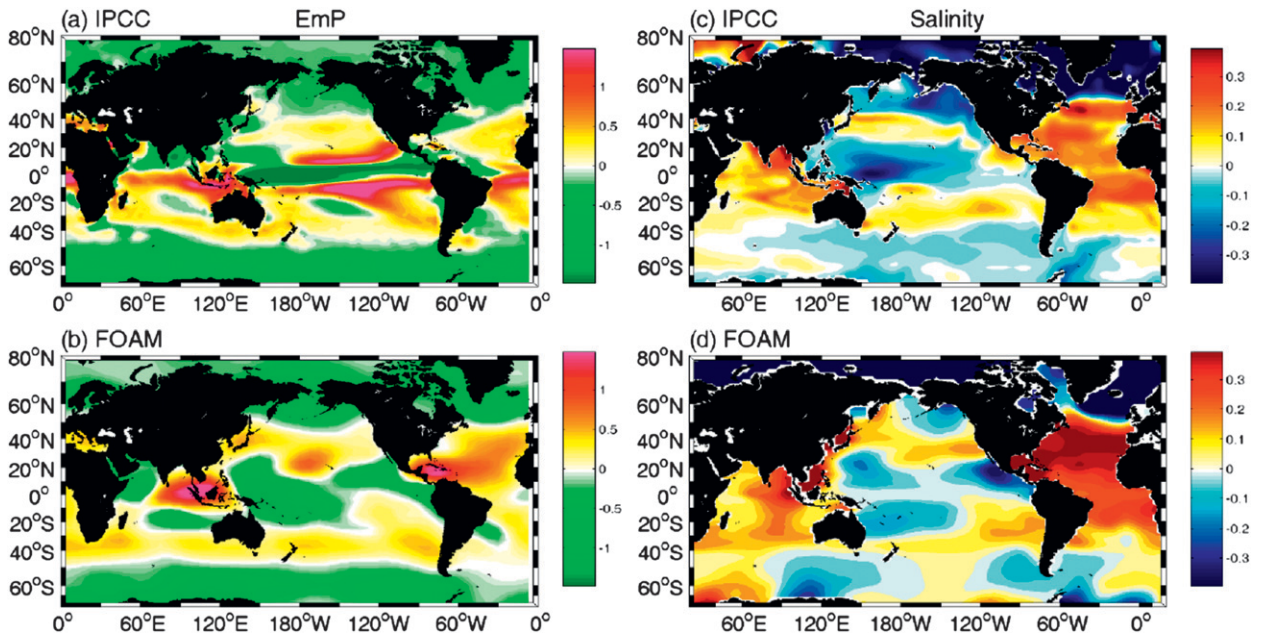


FIG. 1. (a) Ensemble mean of EmP differences between 2CO_2 run and CTRL from 15 models participating in the Coupled Model Intercomparison Project phase 3 and used for the IPCC AR4. Unit is mm day^{-1} . (c) As in (a), but for surface salinity; (b) EmP; and (d) surface salinity differences between FOAM 2CO_2 run and CTRL. Units for EmP and surface salinity are mm day^{-1} and psu, respectively.

3. Results

a. Global mean response

Forced by the sudden onset of CO_2 doubling, the global mean SST increases gradually in the first 100 yr and then reaches equilibrium (Fig. 2a). It can be seen that the SST in the 2CO_2 run increases faster than that in the 2CO_2 _FixEmP run, where the EmP is fixed to the control run climatology (Fig. 2a). A close examination finds that the equilibrium warming reaches $1.4^\circ \pm 0.2^\circ\text{C}$ in the 2CO_2 experiment, but only $1.1^\circ \pm 0.15^\circ\text{C}$ in the 2CO_2 _FixEmP experiment (Fig. 2b). The difference in SST responses between these two runs is about 0.3°C , accounting for about 20% of the simulated warming in the 2CO_2 run. Similarly, the surface air temperature (SAT) response over the land is also amplified by about 15% (Fig. 2b). The experiments readily suggest that the changes in salinity due to EmP changes in response to CO_2 rising tend to amplify the amplitude of SST warming.

The amplification due to changes in EmP in a warm climate can be understood as follows: the intensification of EmP in response to CO_2 rising leads to a shoaling of the mixed layer, a trapping of the heating in the upper ocean, and therefore an amplification of SST warming. To examine the mechanisms contributing to the amplification effect, a mixed layer heat budget analysis is conducted for each group run. The heat budget analysis is based on the following temperature equation:

$$\frac{\partial T}{\partial t} = -u\frac{\partial T}{\partial x} - v\frac{\partial T}{\partial y} - w\frac{\partial T}{\partial z} + \frac{\text{HFLX}}{\rho C_p h} + \text{Mix}, \quad (1)$$

which includes, from left to right, local temperature change, advection, heat flux forcing (HFLX: heat flux, ρ : density, C_p : ocean specific heat, h : mixed layer depth), and mixing term (estimated as the residual, which includes both horizontal and vertical diffusions, convection, etc.). It is seen that the net heat flux term tends to warm the SST in both groups due to the greenhouse gas effect, while the oceanic mixing term plays a damping role to diverge surface warming to the subsurface. The heat flux warming effect is largely associated with the radiative flux as a result of atmospheric feedbacks, while the turbulent heat flux tends to damp the warming due to the increased wind speed, moisture, and air-sea temperature difference (Fig. 2b). A further examination finds that the ocean gains more radiative heat flux in the 2CO_2 run than the 2CO_2 _FixEmP run, implying a stronger positive atmospheric feedback in the 2CO_2 run. In addition to the strong atmospheric feedback, the cooling effect due to the vertical mixing in the 2CO_2 run is also weaker in the 2CO_2 run, which should help sustain the warmer SST (Fig. 2b). This reduced mixing cooling effect is also indicated by the change of the mixed layer depth. We calculate the changes in the globally averaged mixed layer depth, defined as the depth where the difference with the potential density at

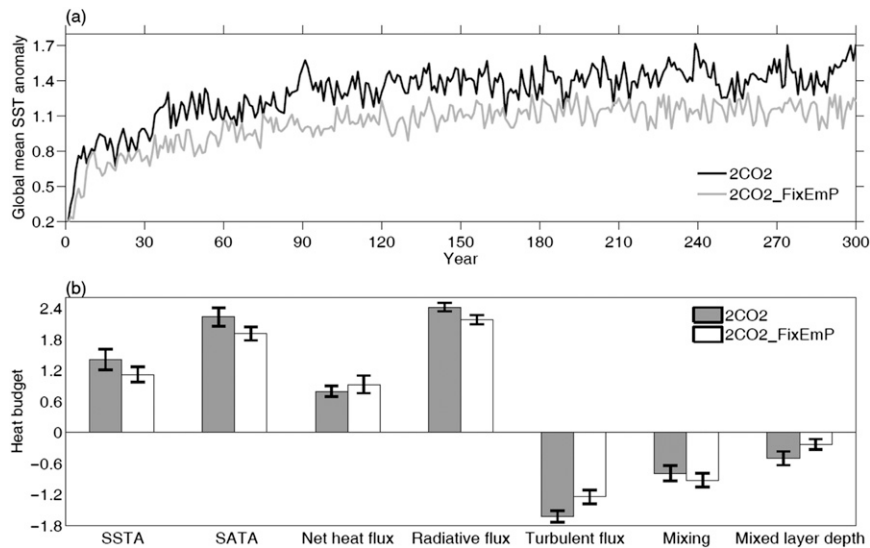


FIG. 2. (a) Time series of global mean SST changes in 2CO_2 run and $2\text{CO}_2_{\text{FixEmP}}$ run. Unit is $^{\circ}\text{C}$. (b) Global mean SST response (SSTA), surface air temperature response (SATA), and mixed layer depth averaged in the last 100 yr. Heat budget terms include heat flux (net, radiative, and turbulent fluxes) and mixing (Mixing) in 2CO_2 run and $2\text{CO}_2_{\text{FixEmP}}$ run. Units for SSTA, SATA, heat flux, mixing, and mixed layer depth are $^{\circ}\text{C}$, $^{\circ}\text{C}$, W m^{-2} , W m^{-2} , and $\text{m}(\times 30)$, respectively.

the first layer equals 0.125 kg m^{-3} , and find that the mixed layer depth becomes shallower in both groups with a magnitude of 7 m in the $2\text{CO}_2_{\text{FixEmP}}$ run and 15 m in the 2CO_2 run (Fig. 2b). Overall, the shallowing of the mixed layer depth in a warm climate can be attributed to the intensification of the ocean stratification and the subsequent decrease of the vertical mixing. A more substantial shoaling of the mixed layer depth in the 2CO_2 run is due to the EmP-induced salinity changes in high latitudes, which will be discussed in next section.

b. Zonal mean response

The zonal mean SST response displays a distinct latitudinal dependence (Fig. 3a). In general, three common characteristics are identified in both groups. First, both groups exhibit a warmer SST response over the higher latitudes than in the lower latitudes (Fig. 3a), with an exception north of 60°N in the 2CO_2 run. This high-latitude amplification has been suggested to be associated with snow-ice albedo feedback as well as dynamical feedback in the ocean and atmosphere (e.g., Cubasch et al. 2001; Cai and Lu 2007; Alexeev et al. 2005). Second, the warming is stronger over the Northern Hemisphere than the Southern Hemisphere due to the larger land coverage in the Northern Hemisphere. Third, a weak warming peak occurs in the equatorial region, which is attributed to the weaker evaporation background in the tropics than in the subtropics, as proposed by Liu et al. (2005) and Xie et al. (2010). The zonal mean of the

mixed layer depth also displays a distinct pattern with a deepening in the subtropics, shoaling in the high latitudes, and no change in the tropics (Fig. 3d). The maximum changes in the mixed layer depth range from about -65 to 35 m, leading to a reduction of the global mean mixed layer depth (Fig. 2b).

Differences in the latitudinal distribution of SST warming between these two experiments are also remarkable. Consistent with the global mean, the SST response is warmer in the 2CO_2 run than the $2\text{CO}_2_{\text{FixEmP}}$ run at most of the latitudes except north of 60°N (Fig. 3a). This exception (strong cooling anomaly) is associated with anomalous horizontal and meridional advection over the Atlantic Ocean (to be discussed in the next section), which leads to a weak polar amplification in the Northern Hemisphere compared to the $2\text{CO}_2_{\text{FixEmP}}$ run. The maximum differences in SST responses occur in the midlatitudes, with a magnitude up to 0.6°C in the Northern Hemisphere and 1°C in the Southern Hemisphere (Fig. 3a). The excessive warming in the 2CO_2 experiment can also be seen in the subsurface ocean, especially over the high latitudes, (Fig. 3b) due to a reduction of the vertical mixing. It is noted that the warming in the subsurface is stronger than in the surface in the Northern Hemisphere and tropics (Fig. 3b). This phenomenon disappears if we average the temperature difference only in the Pacific (not shown), suggesting the role of the meridional overturning circulation in the Atlantic. The temperature pattern in the

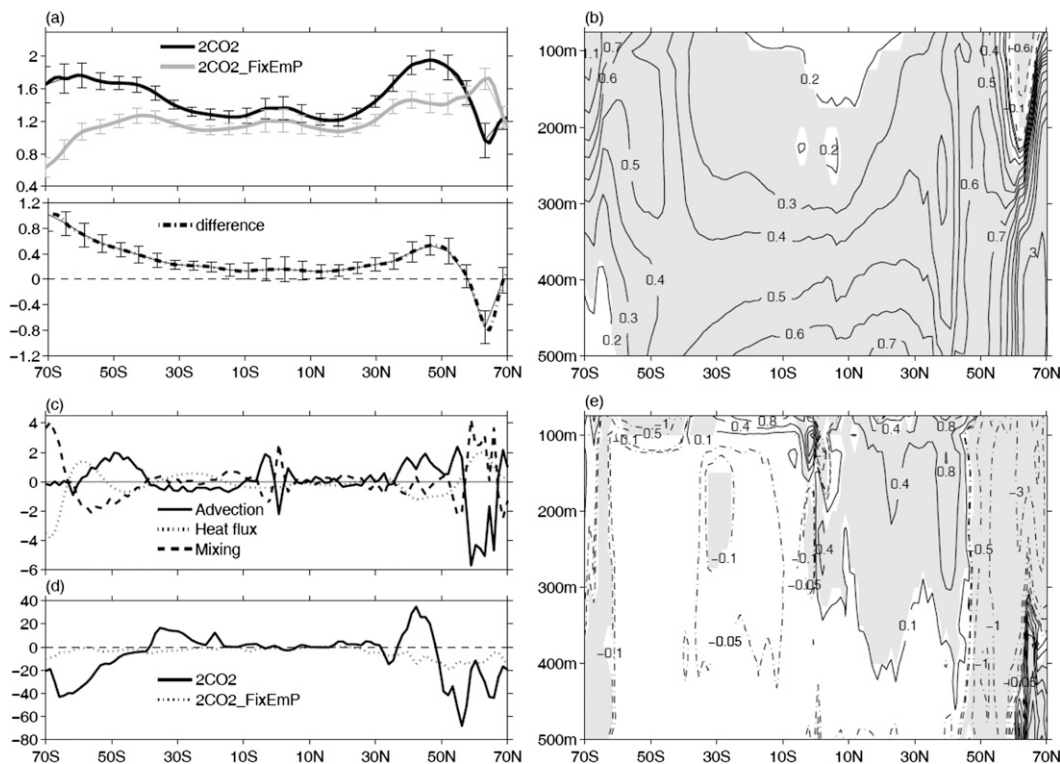


FIG. 3. (a) Zonal mean SST response in 2CO_2 run (solid black line) and $2\text{CO}_2_{\text{FixEmP}}$ run (solid gray line) as well as their differences ($2\text{CO}_2 - 2\text{CO}_2_{\text{FixEmP}}$) (dashed black line). Unit is $^{\circ}\text{C}$. Short vertical lines indicate the 99% confidence level based on a Student's t test. (b) Latitude–depth diagram of subsurface temperature differences between 2CO_2 run and $2\text{CO}_2_{\text{FixEmP}}$ run. Unit is $^{\circ}\text{C}$. (c) Zonal mean mixed layer depth changes in 2CO_2 run (solid black line) and $2\text{CO}_2_{\text{FixEmP}}$ run (solid gray line), (d) Differences of each term in heat budget analysis between the two group experiments. Unit is W m^{-2} . (e) Latitude–depth diagram of meridional velocity differences between 2CO_2 run and $2\text{CO}_2_{\text{FixEmP}}$ run. Unit is m s^{-1} . Gray shaded area exceeds 90% significance level.

subpolar ocean with cooling in the surface and warming in the subsurface is conjectured to be associated with a weakened Atlantic thermohaline circulation in the 2CO_2 run (to be discussed and verified in the next section) (e.g., Manabe and Stouffer 1995).

Relative to the 2CO_2 experiment, the changes of the mixed layer depth in the $2\text{CO}_2_{\text{FixEmP}}$ run is much weaker (Fig. 3d). In general, the different responses in the zonal mean SST and the mixed layer depth in the 2CO_2 and $2\text{CO}_2_{\text{FixEmP}}$ runs suggest an important role of the EmP-induced salinity changes in modulating the warm anomalies through changes of ocean dynamic processes.

To further assess the various effects determining the latitudinal differences, a latitudinal mean mixed layer heat budget analysis is also performed. The warmer SST response over the midlatitudes of both hemispheres in the 2CO_2 experiment is largely associated with anomalous meridional advection (Fig. 3c). From the differences in the zonal mean of the meridional velocity (Fig. 3e), it can be seen that the anomalous poleward flow prevails

over the band of 30° – 50°N , leading to a warm meridional advection and therefore a warmer SST. This poleward flow is due to an increase of salinity in the midlatitudes, which leads to an increase of density, sinking of water, and thus a convergence of mass flux in the upper ocean (Zhang et al. 2011b). North of 55°N , the freshening leads to a reduction of the vertical mixing and a shallower mixed layer, sustaining warming in the deep ocean (Fig. 3b). However, in the upper ocean, the cold advection due to the salinity-driven equatorward anomalous flow significantly reduces the surface warming in high latitudes. This is different in the Southern Hemisphere, where the salinity-induced warming occurs in high latitudes (Figs. 3a,b). The freshening in the southern high latitudes helps trap the CO_2 -induced warming in the surface layer, leading to anomalous easterly winds through ocean–atmosphere coupling and poleward Ekman warm advection (e.g., Ma and Wu 2011). Therefore, both the meridional advection and vertical mixing contribute to the latitudinal pattern of the warmer SST anomalies in the 2CO_2 run (more so than that in the $2\text{CO}_2_{\text{FixEmP}}$ run).

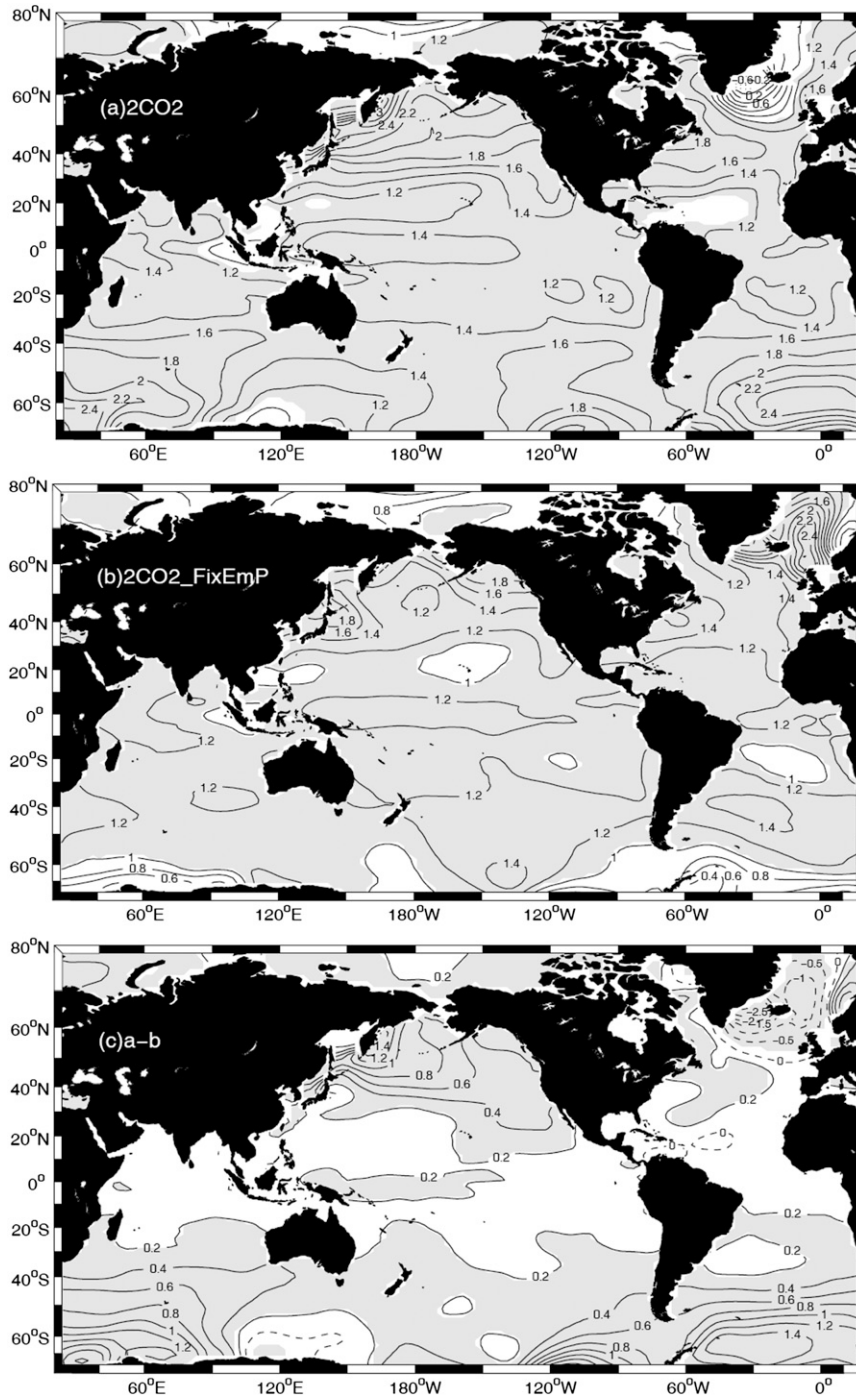


FIG. 4. Annual mean SST response in (a) 2CO_2 run, (b) 2CO_2 _FixEmP run, and (c) their differences. Unit is $^{\circ}\text{C}$. Gray shaded area exceeds 90% significance level.

c. SST spatial pattern and formation mechanisms

1) PACIFIC RESPONSE

The analysis above suggests that the freshwater flux changes in global warming can further sustain the

warming. We turn to a different oceanic basin to examine the warming patterns and the effects of regional ocean dynamics. Over the Pacific Ocean, the warming in the Northern Hemisphere is stronger than that in the Southern Hemisphere in the 2CO_2 run (Fig. 4a), while it

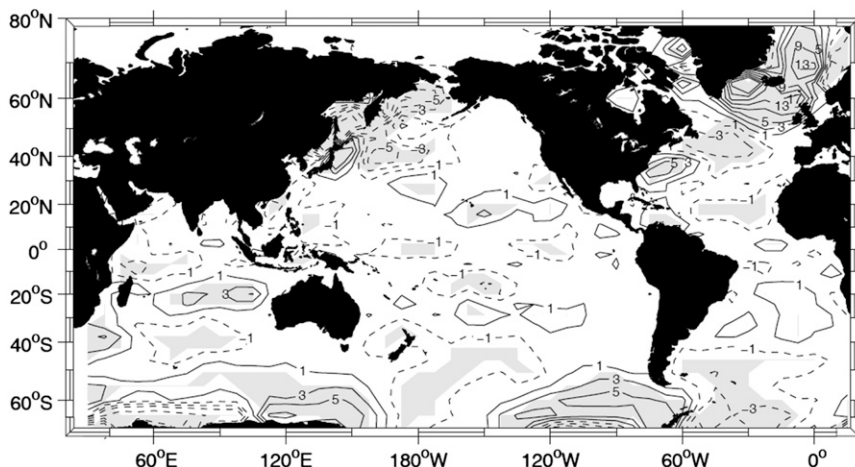


FIG. 5. Annual mean heat flux differences between 2CO_2 run and 2CO_2 _FixEmP run. Unit is W m^{-2} . Gray shaded area exceeds 90% significance level.

is nearly comparable in the 2CO_2 _FixEmP run, in which the changes of the EmP are suppressed (Fig. 4b). The maximum increase of the warming due to the freshwater effects occurs in the subpolar North Pacific with a maximum of 1.4°C (Fig. 4c). The basin average reaches 0.8°C in the North Pacific but only 0.2°C in the South Pacific (Fig. 4c).

The excessive warming in the 2CO_2 run over the North Pacific cannot be explained by surface net heat flux (here, net heat flux change is dominated by turbulent heat flux), which plays a damping effect (Fig. 5). This points to the roles of oceanic dynamics. With a doubling of CO_2 concentration, the subtropical gyre in the North Pacific is intensified and expands northward (Fig. 6a), while in the absence of the EmP changes, the anomalous currents become less significant (Fig. 6b). As a result, the changes of freshwater flux in response to the CO_2 doubling play a critical role in the intensification of the subtropical gyre over the North Pacific (Fig. 6c).

It is noted that the strengthening of the subtropical gyre in the 2CO_2 run cannot be explained by the wind changes. Surface wind responses in both groups are characterized by anticyclonic anomalies straddling the mean position of the westerlies (Figs. 7a,b), indicating a poleward shift of the jet stream under the greenhouse gas forcing (Fu et al. 2006; Quan et al. 2004; Mitas and Clement 2006; Seidel and Randel 2007; Lu et al. 2007). The difference in the surface wind between the 2CO_2 run and the 2CO_2 _FixEmP run exhibits a dipole structure over the North Pacific (Fig. 7c), with a strong cyclonic wind in the north and a weak anticyclonic wind in the south, leading to positive (negative) wind stress curl anomalies in the north (south) (Fig. 8a). The corresponding Sverdrup streamfunction is characterized

by a cyclonic circulation in the midlatitudes (Fig. 8b), which should slow down the subtropical gyre, opposite to what has been seen in Fig. 6c.

The intensification of the subtropical gyre in the North Pacific can be attributed to the salinity changes due to EmP changes in response to global warming. Here, the sea surface salinity response in the 2CO_2 run is characterized by freshening in the high latitudes and the tropics and salinification in the subtropics, manifesting the intensified water cycle in global warming (Figs. 1c,d) (Cubasch et al. 2001; Held and Soden 2006). Over the North Pacific, the negative salinity anomaly in the western subtropics leads to a reduction of seawater density, a rising (deepening) of sea surface height (isopycnals), and thus anticyclonic (cyclonic) circulation in the upper (lower) ocean controlled by geostrophic adjustment (Fig. 9) (Zhang et al. 2011a). This salinity-forced baroclinic flow can penetrate down to 2000 m, reflecting a high-order baroclinic mode adjustment (Liu 1999).

In the South Pacific, there is a dipole wind pattern east of Australia, with a weak cyclonic (negative curl) in the west and a strong anticyclonic (positive curl) in the central region (Figs. 7c, 8a), favoring a cyclonic circulation to the east of Australia as well as a southward western boundary current (Fig. 8b). Therefore, the wind-driven currents east of Australia seem to contribute to part of the southward flow in Fig. 6c. In addition, the westerly anomalies in the high latitudes are substantially weakened in the presence of EmP changes (Fig. 7c), which leads to an anomalous westward flow (Fig. 6c), anomalous southward surface Ekman advection, and hence warmer SST in the higher latitudes (Fig. 4c). The easterly anomalies induced by the EmP changes reflect a coupled ocean–atmosphere feedback in southern high

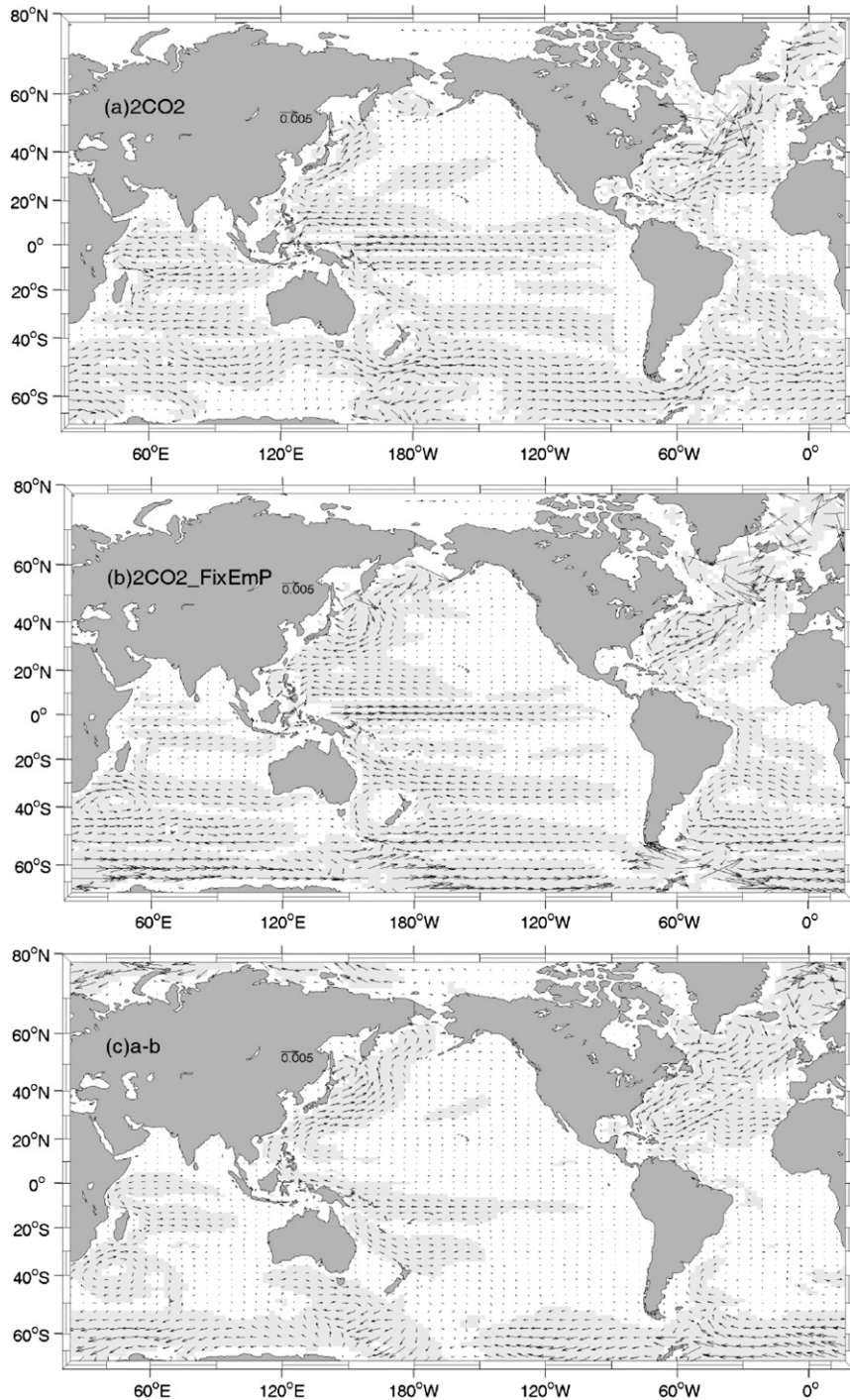


FIG. 6. As in Fig. 4, but for ocean currents averaged in the upper 200 m. Unit is m s^{-1} .

latitudes (e.g., Ma and Wu 2011). Similar to the Northern Hemisphere, low salinity over the southwestern subtropics can also induce an anticyclonic circulation, leading to an anomalous southward western boundary current along the east coast of Australia, as displayed in Fig. 6c.

2) ATLANTIC RESPONSE

The Atlantic Ocean SST response is quite different from that in the Pacific Ocean, with a relatively warmer SST response in the Southern Hemisphere than that in the Northern Hemisphere in the 2CO_2 experiment

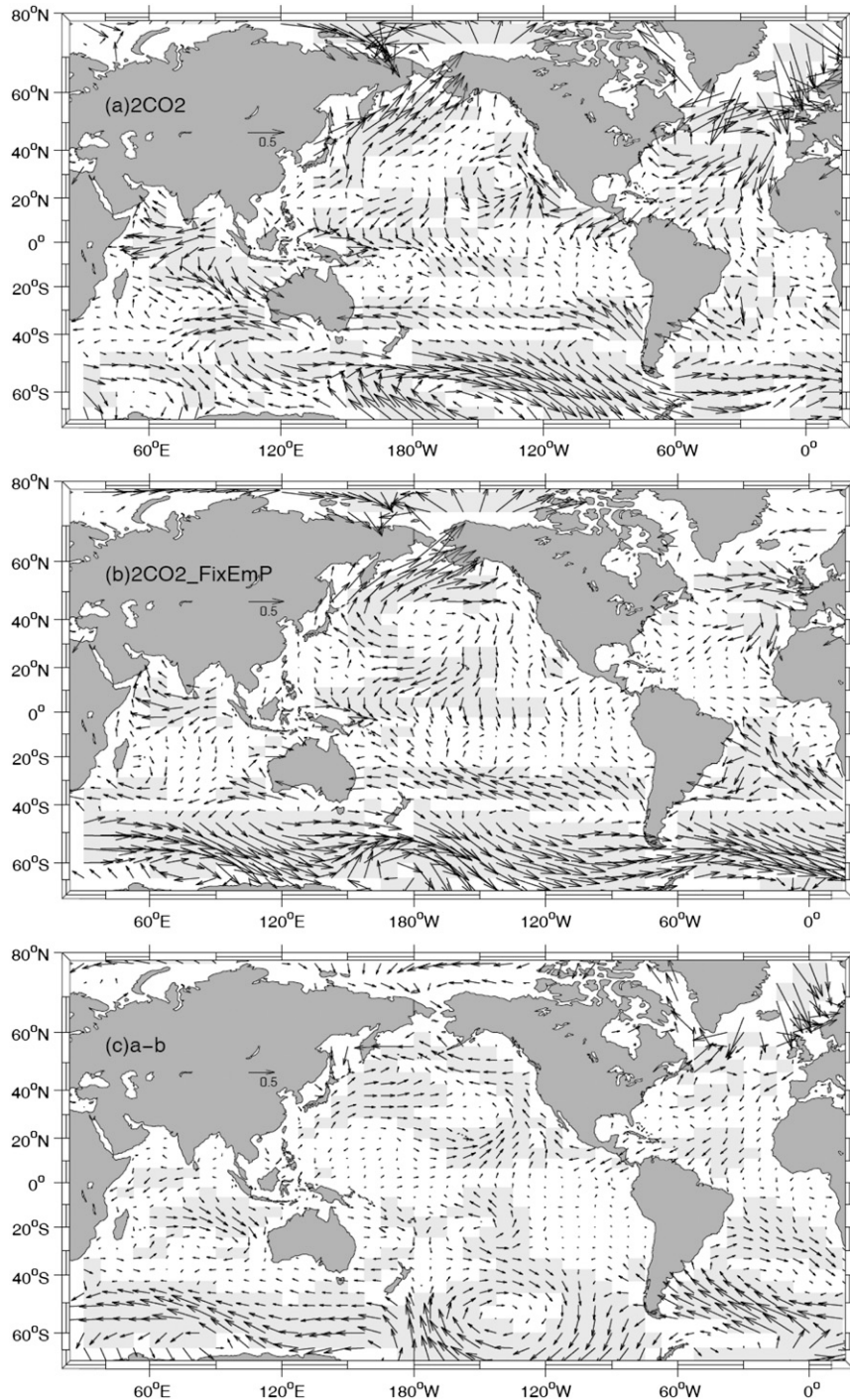


FIG. 7. As in Fig. 4, but for surface wind response. Unit is m s^{-1} .

(Fig. 4a). As the EmP is fixed, the hemispheric asymmetry disappears, although there are strong warm anomalies east of Greenland (Fig. 4b). The Northern–Southern Hemispheric asymmetric SST response is largely associated with the change of the Atlantic meridional overturning circulation (AMOC).

The salinity response over the Atlantic Ocean in the 2CO_2 run is characterized by an increase in the subtropics and tropics and a decrease over the high latitudes (Fig. 1d), consistent with some observations (e.g., Curry et al. 2003; Curry and Mauritzen 2005). Therefore, it can be expected that the AMOC will be weakened in the

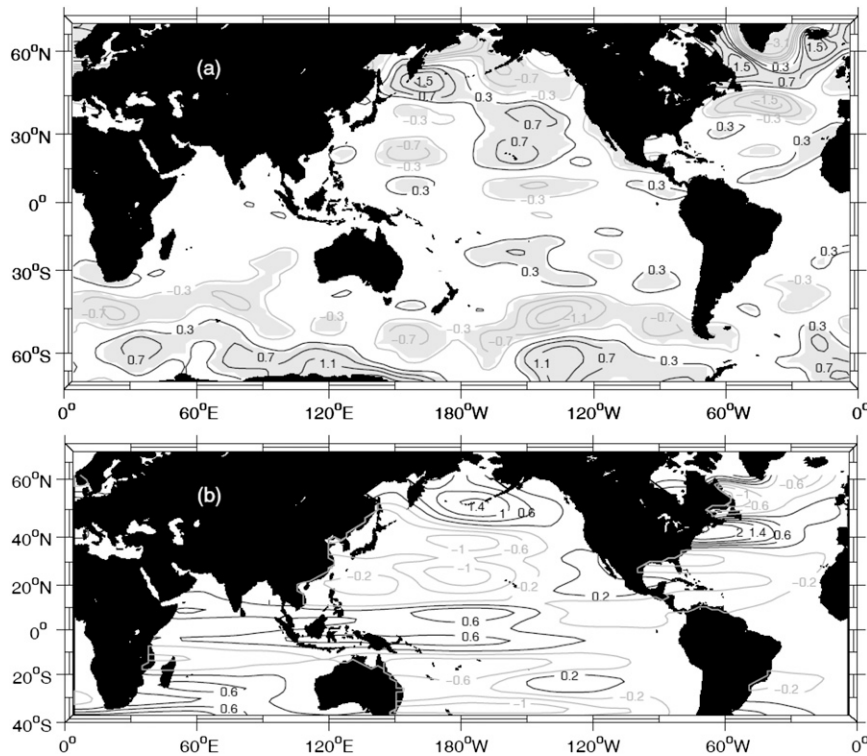


FIG. 8. (a) Differences of wind stress curl response between 2CO_2 and 2CO_2 _FixEmP runs. (b) Corresponding barotropic streamfunction derived from the Sverdrup relation. Units for wind stress curl and streamfunction are N m^{-3} and Sv ($1 \text{ Sv} = 10^6 \text{ m}^3 \text{ s}^{-1}$), respectively.

2CO_2 run. As shown in Fig. 10b, the strength of the AMOC decreases by about 30% at 55°N (Figs. 10a,b). Consequently, the poleward heat transport is significantly reduced, especially over the Northern Hemisphere (Fig. 10d), leading to warming in the South Atlantic, stronger than that in the North Atlantic. As the EmP is fixed, the AMOC as well as the poleward heat transport change less significantly (Figs. 10c,d), leading to a relatively uniform warming over both the North and South Atlantic. Therefore, salinity change plays an important role in regulating the hemispheric SST responses to global warming over the Atlantic Ocean.

The salinity changes due to the EmP changes over the North Atlantic Ocean can not only modulate the AMOC strength but also induce a remarkable adjustment of the horizontal gyre circulation. The anomalous currents in the upper 200 m over the subtropical North Atlantic Ocean are characterized by a cyclonic gyre circulation (Fig. 6a), which appears to be inconsistent with the wind stress changes (Fig. 7a). In the absence of the EmP changes, the anomalous currents turn to an anticyclonic circulation (Fig. 6b), consistent with the wind changes (Fig. 7b). Therefore, the anomalous cyclonic circulation in the subtropical North Atlantic is attributed

to the salinity changes. As shown in Fig. 1d, a dipole salinity anomaly dominates over the North Atlantic Ocean, with the negative anomaly in the north and the positive anomaly in the south. The corresponding circulation associated with the salinity distribution is an

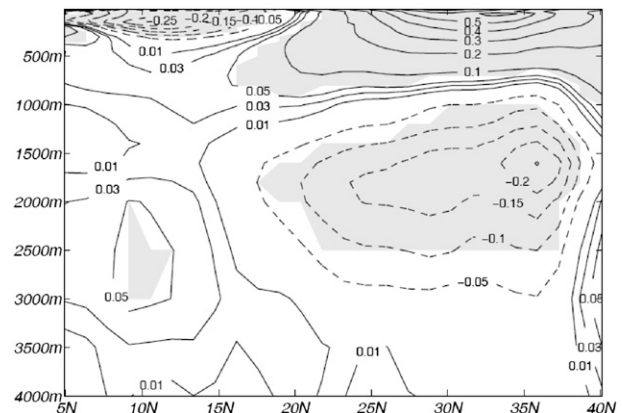


FIG. 9. Zonal velocity differences ($2\text{CO}_2 - 2\text{CO}_2$ _FixEmP) averaged between 120° and 160°E . Unit is cm s^{-1} . Gray shaded area exceeds 90% confidence level.

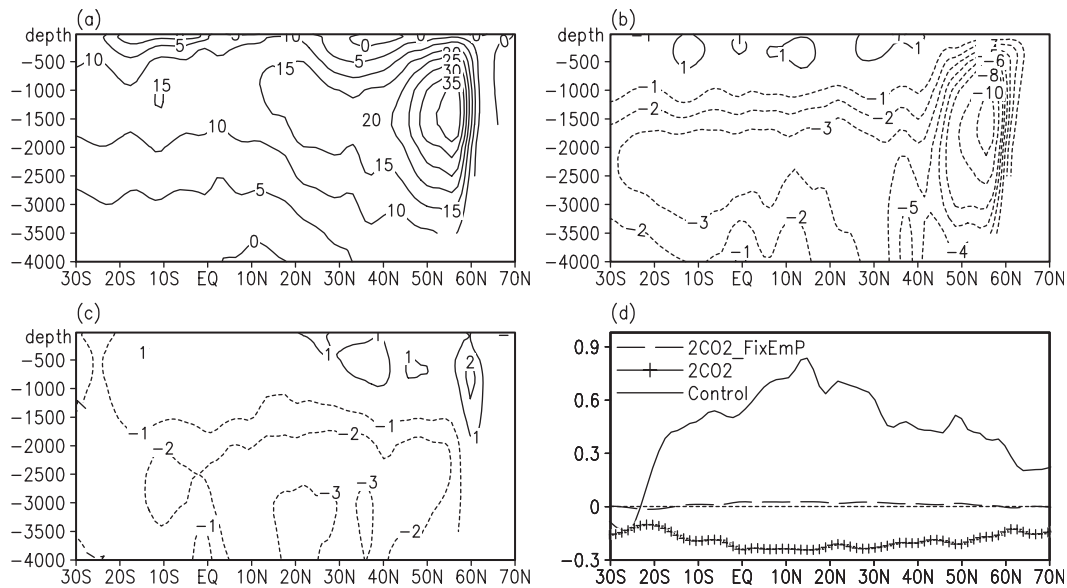


FIG. 10. (a) Latitude–depth profile of climatological meridional streamfunction denoting the AMOC in CNTRL. (b) AMOC changes in 2CO₂ run. (c) AMOC changes in 2CO₂_FixEmP run. (d) Mean poleward heat transport and its changes in 2CO₂ run and 2CO₂_FixEmP run. Unit is PW (10^{15} W m^{-2}).

anomalous cyclonic gyre over the positive salinity anomaly and an anticyclonic gyre over the negative salinity anomaly (Figs. 6a,c) (Zhang et al. 2011b). The cyclonic circulation anomalies in the subtropics reduce (enhance) the warming in the northeast (southwest) through southward (northward) cold (warm) advection, while the anomalous anticyclonic circulation in the subpolar North Atlantic, albeit weak, leads to southwest cold advection, reducing the warming to the east and south of Greenland (Figs. 4a,b).

4. Summary and discussion

This paper studied the role of freshwater flux changes in regulating the SST responses to global warming using coupled model simulations. It is found that the salinity changes due to the amplification of freshwater flux tend to amplify the warming of the global mean SST by about 30%. The explanations are as follows: the salinity change in response to a doubling of the CO₂ concentration is characterized by a freshening in the tropics

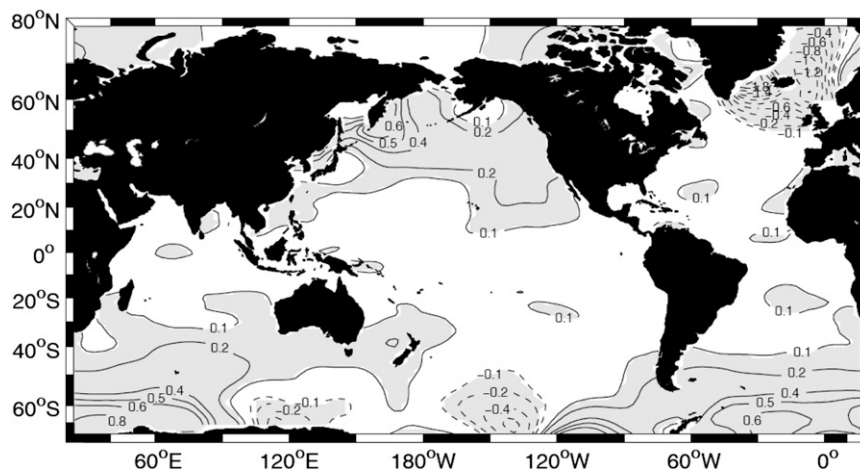


FIG. 11. SST response with EmP fixed to 2CO₂ climatology but with a normal CO₂ concentration (355 ppm).

and high latitudes and a salinification in the subtropics, a manifestation of the accelerated water cycle in a warm climate. This should enhance oceanic stratification in high latitudes, reduce vertical mixing and mixed layer depth, and thus trap CO_2 -induced warming in the surface layer.

Atmosphere feedback seems to act as a positive feedback to amplify SST warming in the fully coupled 2CO_2 run. Warmer SST not only increases water vapor in the atmosphere, inducing adownward radiative flux to sustain warm SST, but also reduces low clouds in the low troposphere, which in turn increases more solar shortwave radiation to warm the ocean (not shown).

To further assess the roles of the oceanic dynamics and atmospheric feedbacks associated with freshwater flux changes in global warming, we perform another experiment, in which EmP is fixed to 2CO_2 run climatology but with the normal CO_2 concentration. In this case, the effects of global warming-induced freshwater change still exist but atmospheric feedbacks associated with global warming are eliminated. It is found that the SST response is broadly consistent with that in the presence of CO_2 doubling, with a significant warming in the mid-latitudes (Fig. 11 vs Fig. 4c), suggesting the important role of ocean dynamics. However, the amplitude of the SST response is weaker in the absence of atmospheric feedbacks associated with global warming.

The latitudinal distribution of SST changes due to the EmP effects in a warm climate can be summarized as follows (Fig. 12). An accelerated water cycle in a warm climate leads to negative (positive) surface salinity anomalies (SSAs) in the high latitudes (the subtropics and midlatitudes). In the Northern Hemisphere, the freshening leads to a reduction of vertical mixing, which should help trap CO_2 -induced warming in the surface layer, slow down the meridional overturning circulation,

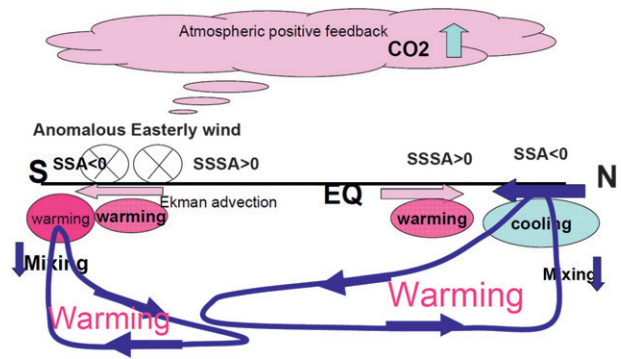


FIG. 12. Schematic diagram of processes associated with EmP changes in a warm climate.

and thus the warming of the deep ocean. Meanwhile, the latitudinal difference in the surface salinity also leads to anomalous convergent flows in the midlatitudes, which amplify the warming in the midlatitudes but reduce the warming in the high latitudes. In the Southern Hemisphere, the freshening in the high latitudes traps CO_2 -induced warming in the surface layer and reduces bottom water formation, leading to warming in both the surface and deep ocean. The warming in the surface triggers easterly anomalies through local coupled ocean-atmosphere feedback, inducing poleward anomalous Ekman warm advection. This warm advection significantly offsets the salinity-driven equatorward cold advection as seen in the Northern Hemisphere's high latitudes and thus sustains the warming in the Southern Hemisphere's high latitudes.

Our conclusion seems to contradict the results of Williams et al. (2007), who suggest that the amplified water cycle in a warm climate tends to suppress oceanic warming and thus provides a negative feedback to global warming. To examine whether the results are model

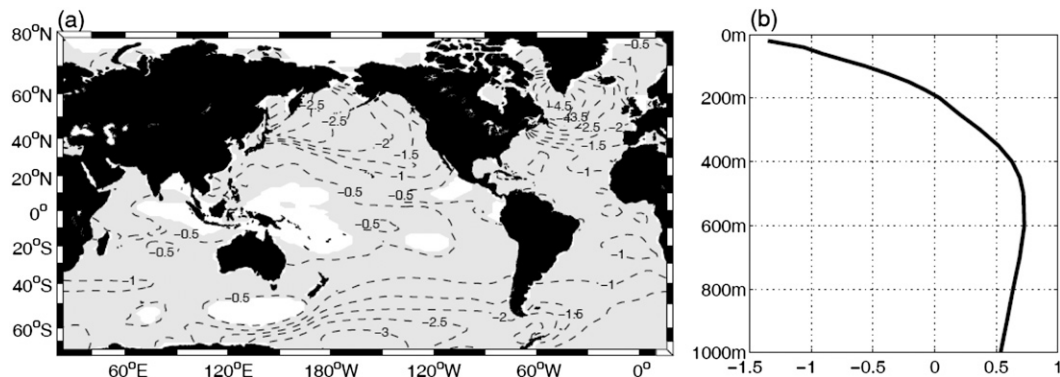


FIG. 13. (a) Annual mean SST responses in the experiment with a doubling of freshwater flux without a doubling of CO_2 concentration. Gray shaded area exceeds 90% confidence level based on the t test. (b) Vertical profile of global mean temperature response averaged in the global ocean. Unit is $^{\circ}\text{C}$.

dependent, we repeat their experiments with FOAM, in which the freshwater flux is doubled but without increasing the CO₂ concentration. The model produces cooling globally with more intensive cooling over the high latitudes, consistent with their modeling results (Fig. 13). The cooling is largely trapped in the upper 200 m with warming beneath, suggesting an enhanced vertical mixing and downward heat diffusion. The reasons why a doubling of the freshwater flux cannot mimic the effects of the freshwater flux in global warming are complicated, which may be attributed to regional structures of the freshwater flux and different feedbacks in global warming. By excluding the possibility of model dependence, we argue that the freshwater flux may amplify rather than suppress global warming. Our study suggests that monitoring and understanding of long-term changes of oceanic salinity are important for the projection of future climate changes.

Acknowledgments. This work was supported by the Major Project of National Science Foundation of China (Grants 40890150 and 40890155), the National Science Foundation for Distinguished Young Scholars of China (Grant 40788002), and Scholarship Award for Excellent Doctoral Student granted by Ministry of Education. Discussions with Drs. Rong Zhang and S.-P. Xie were helpful.

REFERENCES

- Alexeev, V. A., P. L. Langen, and J. R. Bates, 2005: Polar amplification of surface warming on an aquaplanet in “ghost forcing” experiments without sea ice feedbacks. *Climate Dyn.*, **24**, 655–666.
- Cai, M., and J. Lu, 2007: Dynamical greenhouse-plus feedback and polar warming amplification. Part II: Meridional and vertical asymmetries of the global warming. *Climate Dyn.*, **29**, 375–391.
- Cubasch, U., and Coauthors, 2001: Projections of future climate change. *Climate Change 2001: The Scientific Basis*, J. T. Houghton et al., Eds., Cambridge University Press, 525–582.
- Curry, R., and C. Mauritzen, 2005: Dilution of the northern North Atlantic Ocean in recent decades. *Science*, **308**, 1772–1774.
- , B. Dickson, and I. Yashayaev, 2003: A change in the freshwater balance of the Atlantic Ocean over the past four decades. *Nature*, **426**, 826–829.
- Dai, A., I. Y. Fung, and A. D. Del Genio, 1997: Surface observed global land precipitation variations during 1900–88. *J. Climate*, **10**, 2943–2962.
- Fedorov, A. V., R. Pacanowski, S. G. Philander, and G. Boccaletti, 2004: The effect of salinity on the wind-driven circulation and the thermal structure of the upper ocean. *J. Phys. Oceanogr.*, **34**, 1949–1966.
- , M. Barreiro, G. Boccaletti, R. Pacanowski, and S. G. Philander, 2007: The freshening of surface waters in high latitudes: Effects on the thermohaline and wind-driven circulations. *J. Phys. Oceanogr.*, **37**, 896–907.
- Fu, Q., C. M. Johanson, J. M. Wallace, and T. Reichler, 2006: Enhanced mid-latitude troposphere warming in satellite measurements. *Science*, **312**, 1179–1179.
- Hall, A., and S. Manabe, 1999: The role of water vapor feedback in unperturbed climate variability and global warming. *J. Climate*, **12**, 2327–2346.
- Held, I. M., and B. J. Soden, 2006: Robust responses of the hydrologic cycle to global warming. *J. Climate*, **19**, 5686–5699.
- Huang, B., and V. M. Mehta, 2005: Response of the Pacific and Atlantic Oceans to interannual variations in net atmospheric freshwater. *J. Geophys. Res.*, **110**, C08008, doi:10.1029/2004JC002830.
- , —, and N. Schneider, 2005: Oceanic response to idealized net atmospheric freshwater in the Pacific at the decadal time scale. *J. Phys. Oceanogr.*, **35**, 2467–2486.
- Jacob, R.L., 1997: Low frequency variability in a simulated atmosphere ocean system. Ph.D. thesis, University of Wisconsin—Madison, 155 pp.
- Liu, Z., 1999: Forced planetary wave response in a thermocline gyre. *J. Phys. Oceanogr.*, **29**, 1036–1055.
- , J. Kutzbach, and L. Wu, 2000: Modeling climatic shift of El Niño variability in the Holocene. *Geophys. Res. Lett.*, **27**, 2265–2268.
- , S. Vavrus, F. He, N. Wen, and Y. Zhong, 2005: Rethinking tropical ocean response to global warming: The enhanced equatorial warming. *J. Climate*, **18**, 4684–4700.
- Lu, J., G. A. Vecchi, and T. Reichler, 2007: Expansion of the Hadley cell under global warming. *Geophys. Res. Lett.*, **34**, L06805, doi:10.1029/2006GL028443.
- Lukas, G., and F. Santiago-Mandujano, 2008: Interannual to interdecadal salinity variations observed near Hawaii: Local and remote forcing by surface freshwater fluxes. *Oceanography*, **21**, 46–55.
- Ma, H., and L. Wu, 2011: Global teleconnections in response to freshening over the Antarctic ocean. *J. Climate*, **24**, 1071–1088.
- Manabe, S., and R. Stouffer, 1995: Simulation of abrupt climate change induced by freshwater input to the North Atlantic Ocean. *Nature*, **378**, 165–167.
- Mitas, C. M., and A. Clement, 2006: Recent behavior of the Hadley cell and tropical thermodynamics in climate models and reanalyses. *Geophys. Res. Lett.*, **33**, L01810, doi:10.1029/2005GL024406.
- Quan, X., H. F. Diaz, and M. P. Hoerling, 2004: Changes in the tropical Hadley cell since 1950. *The Hadley Circulation: Past, Present, and Future*, H. F. Diaz and R. S. Bradley, Eds., Advances in Global Change Research, Vol. 21, Springer, 85–120.
- Seager, R., and N. Naik, 2010: Thermodynamic and dynamic mechanisms for large-scale changes in the hydrological cycle in response to global warming. *J. Climate*, **23**, 4651–4668.
- Seidel, D. J., and R. J. Randel, 2007: Recent widening of the tropical belt: Evidence from tropopause observations. *J. Geophys. Res.*, **112**, D20113, doi:10.1029/2007JD008861.
- Soden, B. J., 2000: Enlightening water vapor. *Nature*, **406**, 247–248.
- , R. T. Wetherald, G. L. Stenchikov, and A. Robock, 2002: Global cooling after the eruption of Mount Pinatubo: A test of climate feedback by water vapor. *Science*, **296**, 727–730.
- , D. L. Jackson, V. Ramaswamy, M. D. Schwarzkopf, and X. Huang, 2005: The radiative signature of upper tropospheric moistening. *Science*, **310**, 841–844.
- Williams, P. D., E. Guilyardi, R. Sutton, J. Gregory, and G. Madec, 2006: On the climate response of the low-latitude Pacific Ocean to changes in the global freshwater cycle. *Climate Dyn.*, **27**, 593–611.

- , —, —, —, and —, 2007: A new feedback on climate change from the hydrological cycle. *Geophys. Res. Lett.*, **34**, L08706, doi:10.1029/2007GL029275.
- Wong, A. P. S., N. L. Bindoff, and J. A. Church, 1999: Large-scale freshening of intermediate waters in the Pacific and Indian Oceans. *Nature*, **400**, 440–443.
- Wu, L., Z. Liu, R. Gallimore, R. Jacob, D. Lee, and Y. Zhong, 2003: Pacific decadal variability: The tropical Pacific mode and the North Pacific mode. *J. Climate*, **16**, 1101–1120.
- Xie, S.-P., C. Deser, G. A. Vecchi, J. Ma, H. Teng, and A. T. Wittenberg, 2010: Global warming pattern formation: Sea surface temperature and rainfall. *J. Climate*, **23**, 966–986.
- Zhang, L., L. Wu, and J. Zhang, 2011a: Coupled ocean–atmosphere responses to recent freshwater flux changes over the Kuroshio–Oyashio Extension region. *J. Climate*, **24**, 1507–1524.
- , —, and —, 2011b: Simulated response to recent freshwater flux change over the Gulf Stream and its extension: Coupled ocean–atmosphere adjustment and Atlantic–Pacific teleconnection. *J. Climate*, **24**, 3971–3988.
- Zhong, Y., and Z. Liu, 2009: On the mechanism of Pacific multidecadal climate variability in CCSM3: The role of the subpolar North Pacific Ocean. *J. Phys. Oceanogr.*, **39**, 2052–2076.